JOURNAL OF SPACECRAFT AND ROCKETS
Vol. 38, No. 4, July–August 2001

Study of Long Duration Exposure Facility Contaminated Chromic-Acid-Anodized Surfaces

S. L. B. Woll,* V. A. Loebs,† C. S. Phelps,‡ and H. G. Pippin§
Boeing Phantom Works, Seattle, Washington 98124-2499
D. G. Crandall¶
AZ Technologies, Huntsville, Alabama 35806
and
W. H. Kinard**
NASA Langley Research Center, Hampton, Virginia 23681-2199

Contamination plumes that were visible postflight on chromic-acid-anodized experiment tray panels flown on the Long Duration Exposure Facility were examined for content, thickness, and optical property values as a function of location on the panel. The source of the contamination was determined to be a mixture of methyl silicone that was suspected to have outgassed from a tray cover gasket during preflight storage and polyurethane that outgassed from Z306 black paint both preflight and on orbit. Contamination depths on the panels ranged from 40 to 36,000 Å. Changes in solar absorptance and thermal emittance were mathematically modeled as functions of atomic oxygen fluence, solar exposure, and contaminant thickness. Very high correlation was found between discoloration and atomic oxygen exposure. Little correlation was found between discoloration and solar exposure. The atomic oxygen coefficients for the panel models indicated that the optical properties of the contaminated, anodized panels degraded twice as much as the contaminated, untreated brackets. The change in solar absorptance was approximately 0.06 per 1000 Å. This change is less than the rate derived from earlier linear degradation models using temperature data telemetered from operational satellites, which have reported solar absorptance changes of 0.01 per 100 Å.

Nomenclature

R^2 = least-squares correlation coefficient
α = solar absorptance
ε = thermal emittance

Introduction

THE International Space Station (ISS) program has a need to predict optical property degradation for various space-exposed external surfaces over time. As surfaces age in the ISS environment, contamination will build, optical properties will change, and temperatures will rise.

Higher temperatures, in turn, will mean higher power requirements and decreased ISS performance. Models that can predict optical property degradation will be useful in determining when corrective action is required and will assist in scheduling hardware maintenance or replacement missions.

The specific goal of this investigation was to construct models for predicting the optical property changes of silicone-contaminated chromic-acid-anodized surfaces as a function of solar exposure, atomic oxygen fluence, and contaminant thickness. The stored trays from the Long Duration Exposure Facility (LDEF) presented a valuable opportunity to gather postflight data from chromic-acid-anodized hardware. The evidence indicated that the contaminant source was silicone from a gasket used preflight.

The LDEF chromic-acid-anodized (CAA) aluminum surfaces were chosen for examination because it was recognized that CAA surfaces are widely used on ISS and that the LDEF and ISS surfaces were produced by very similar processes. Also, LDEF flew in low Earth orbit for about 5.8 years under conditions representative of expected ISS exposure conditions. The higher inclination of ISS will result in a higher dose of particulate radiation relative to LDEF, but the ranges of atomic oxygen, solar UV radiation impact rates (possibly), and contamination exposures should be similar. In addition, the mixture of contaminants (silicone and carbon-containing polyurethane) is a combination that is likely to occur on ISS as a result of off-gassing of solar arrays and other hardware. Therefore, the data obtained from LDEF surfaces should be highly relevant to predicting the effects of the environment on ISS surfaces.

Small apertures between the truss corners and the LDEF experiment tray overhangs allowed the contaminant surfaces to be exposed to a range of solar and atomic oxygen fluences. Those fluences were known using a previously developed mathematical LDEF model. Thus, the substrate, contaminant and environmental exposures were known and only postflight data collection was necessary to begin the modeling effort.

The LDEF panels were retrieved from storage, and the optical properties were measured at different points across the contamination plumes. The mathematical model was run to determine the solar and atomic oxygen exposures at the same points. Nonlinear regression analysis was then performed on the resulting multivariate data set to model the optical property changes as a function of solar exposure, atomic oxygen fluence, and contaminant thickness.

LDEF

The LDEF, shown in Fig. 1, was a materials experiment that flew in low Earth orbit (LEO) for 69 months.[1] LDEF was deployed from the Space Shuttle STS 41-C at 257 n miles on 7 April 1984. LDEF then flew in a gravity gradient stabilized, fixed orientation of 28.5 deg inclination until retrieved by STS-32 on 12 January 1990 at an altitude of 179 n miles.

The 12-sided experiment was approximately 4.3 m in diameter and 9.1 m long. LDEF frame was an open grid truss structure. Seventy-two experiment trays were mounted on the equally sized openings on the sides, and an additional 14 were mounted on openings at the ends. Figure 2 is a close-up view of the LDEF taken during disassembly at Kennedy Space Center (KSC) that shows the

---

Received 2 December 1999; revision received 11 December 2000; accepted for publication 12 December 2000.

*Senior Specialist Engineer, Non-Metallic Materials Technology, MS 82-94, P.O. Box 3707.

†Process Materials and Component Analyst, Analytical Engineering, MS 3W-50, P.O. Box 3999.

‡Senior Specialist Engineer, Physics, MS 8H-05, P.O. Box 3999.

§Senior Specialist Engineer, Non-Metallic Materials Technology, MS 73-09, P.O. Box 3999. Member AIAA.

¶Optical Engineer, 7047 Old Madison Pike, Suite 300.

**Senior Scientist, MS 188B.

truss structure with mounted experiment trays. On Earth the LDEF weighed 10.5 tons.

The tray locations of each individual experiment were designated with an alphabetical letter and a number. The trays were labeled A through F along the longitudinal direction. The letter G was reserved for the Earth-facing end and H for the space-facing end. The trays were numbered from 1 to 12 in a clockwise direction when facing the Earth end. Figure 3 is a cross section associated with the midsection of the LDEF that includes calculated environmental exposures for the mission.

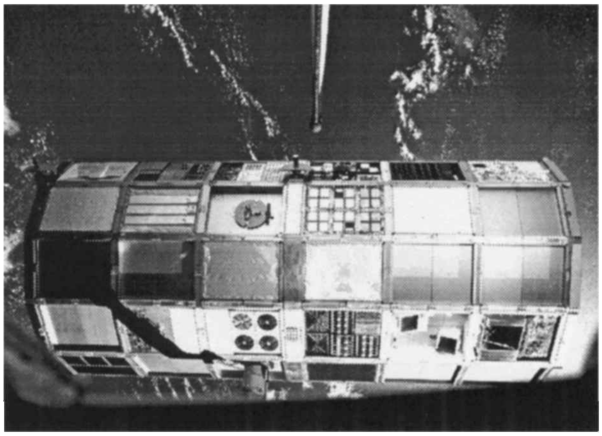

Fig. 1 LDEF as seen from the shuttle cargo bay during retrieval (NASA photograph).

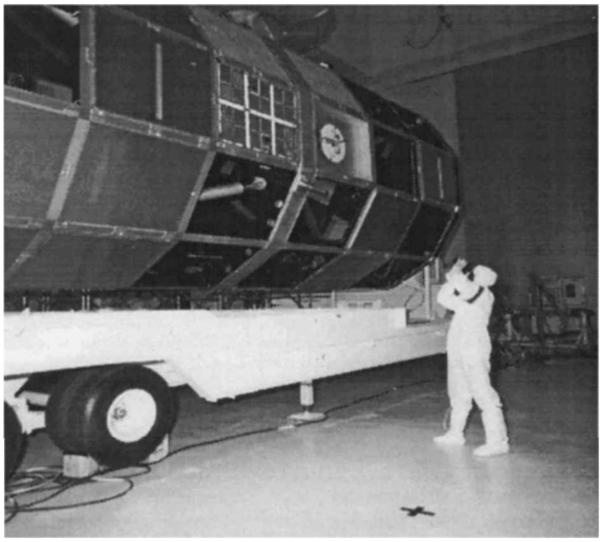

Fig. 2 LDEF truss with mounted experiments during disassembly (NASA photograph).

The trays examined during this study were approximately 34 in. wide × 46 in. long × 12 in. deep. The top half of the exterior of each tray was chromic acid anodized, and the bottom half of each tray was painted with Z306 black polyurethane-based paint. Individual experiment trays were stored prior to the flight for periods of time ranging from several weeks to several years.

Contaminant Source

The trays were stored preflight with aluminum lids that had silicone rubber gaskets along the entire tray perimeters. The trays had attachment tabs, or overhangs, extending along the perimeter of each tray, except at the corners. Preflight, the gaskets at the tray corners had a line-of-sight view to the tray exterior. For flight the gaskets were removed, and the gaps allowed atomic oxygen and solar UV from the environment to interact with the exterior tray surfaces.

Postflight discoloration patterns on the edges of certain tray tabs matched the width and location of the gasket material. Figure 4 is a postflight photograph of Tray A7 with the lid and gasket installed for storage. A plume of discoloration extends from the square tray aperture on the exterior of the tray panel where the surface was exposed to solar and atomic oxygen fluences. Similar postflight contamination plumes were seen in all areas that received significant amounts of atomic oxygen and solar radiation.

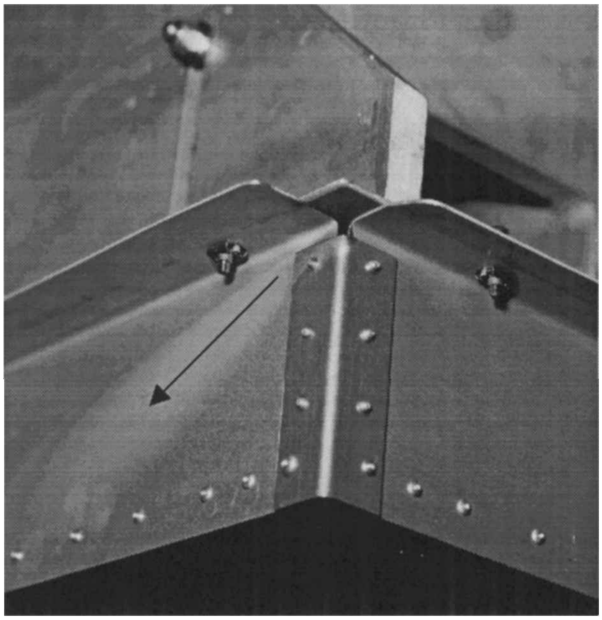

Fig. 4 Postflight contamination on tray A7 (NASA photograph).

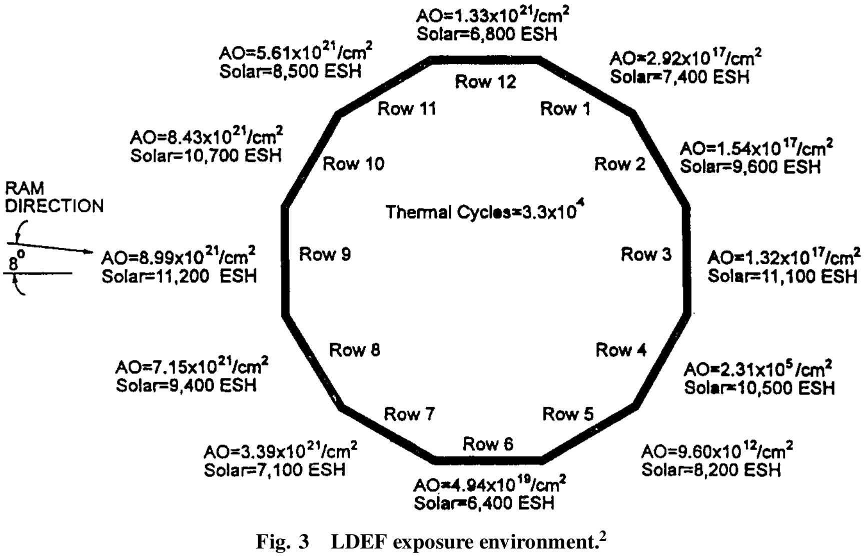

Fig. 3 LDEF exposure environment.[2]

A sample of methyl silicone gasket material was obtained that was believed to be the same material used for the LDEF gaskets. Samples of the gasket material and the plume contamination were submitted for infrared (IR) analysis. The contamination spectrum showed a broad peak between 1000 to 1200 cm^{-1} that is most likely degraded silicone. The peak matched well with the silicone rubber peak in the same region on the gasket spectra. Also, the C—H stretch at 3000 cm^{-1} was found on both spectra. The results of the IR analysis showed that the gasket material tested is most likely the same as the gasket material used and, more importantly, that methyl silicone was the contaminant source.

The spectra also provided an unexpected result. There was a series of peaks between 1300 and 1800 cm^{-1} that is definitely not associated with silicone. Rather, the additional contaminant that was evident matched the spectra of polyurethane. The suspected source of the polyurethane contaminant is the Z306 black paint that was used on the bottom half of the tray panels.

Optical Property Measurements

Potential Artifacts

A concern was raised that postflight conditions and/or exposures could have altered the surfaces of interest. There was a considerable period of time between the return to ground in 1990 and the examination of the contaminated surfaces in 1998. Following postflight examination of the experiments immediately upon return to Earth in early 1990, there were several subsequent examinations that entailed removal of the experiments from the trays at each experimenter's facility. Eventually, the trays were returned to their individually sealed storage containers.

One concern was that the postflight exposure of the tray exterior surfaces to the gasket material may have resulted in additional deposition of silicones onto the aluminum substrates, altering the apparent effects of the preflight and flight exposures. While the LDEF hardware was at KSC, the original gaskets were replaced with fresh gaskets of the same material. After the return of the empty trays, the trays were stored in their individual shipping containers with each lid in place on each tray.

Another concern was that material could have been deposited postflight during the various exposures in experimenter's labs and at NASA Langley Research Center. For example, in December of 1998, the tray shipping containers of interest in this study were opened, and the trays were removed and placed on a laboratory bench prior to measuring optical properties. In the case of two of the three trays chosen for examination, a clear plastic film had been placed between the tray lid and gasket and the corresponding tray. It was unknown whether the plastic film had outgassed and deposited onto the surfaces of interest. On the other hand, the film, where present, provided a barrier to line-of-sight postflight silicone deposition from the gasket.

To address these concerns, optical measurements were made on several trays before and after a solvent wipe with isopropyl alcohol (IPA). Attempts to remove portions of this molecular thin film contaminant for analysis in early 1990 succeeded only after aggressive mechanical abrasion with course sandpaper was used. A previous study indicated that the discolored areas could be expected to be heavily oxidized.[2] Thus, it was thought that the isopropyl alcohol would remove only loose material deposited postflight.

Results of these test measurements are shown in Table 1. In every case except one, the optical property changes were very small with the difference before and after cleaning being within the sensitivity of the instruments. The contaminant layer was well adhered and required chipping to remove. Photographs taken in early 1990 were examined together with the actual surfaces both before and after wiping with IPA. There were no apparent changes in the visual appearance of the discolored areas. The conclusion, therefore, was that postflight contamination, if present, was insignificant and did not affect the optical property measurements. All tray surfaces were subsequently wiped with IPA in the laboratory before measuring optical properties.

Solar Absorptance and Thermal Emissivity Measurements

Solar absorptance and thermal emissivity measurements were made across the contamination plumes on the panels and on the brackets. Measurements on the brackets were made between the rivet holes away from the rivet shadow. Measurements were made on the following tray panels: C8 Earth end, row 11 Earth end, row 11 space end, row 7 Earth end, and row 7 space end. The exact panel location is unknown for the row 11 and row 7 panels. A discrepancy was noted between the photographs taken during disassembly and panels that were removed from storage. Using the set of available disassembly photographs, along with the knowledge that the plume angles would be the same for the same row, the panels were matched to the proper row and end. Figure 5 shows a photograph of the C8 Earth end panel with the bracket superimposed.

Table 1 Effect of IPA wipe on solar absorptance measurements

	Solar absorptance	
Measurement position	Initially	After IPA wipe
C8 Earth end bracket, between		
Holes 1 and 2	0.565	0.559
Holes 2 and 3	0.542	0.528, 0.526
Holes 3 and 4	0.482	0.488
Holes 4 and 5	0.447	0.439
B7 Earth end bracket, between		
Holes 1 and 2	0.540, 0.539	0.538
Holes 2 and 3	0.440	0.436
Holes 3 and 4	0.440, 0.437	0.435
Holes 4 and 5	0.444	0.444
B7 space end panel		
Corner toward row 8, 1	0.375	0.371
Corner toward row 8, 2	0.427	0.420

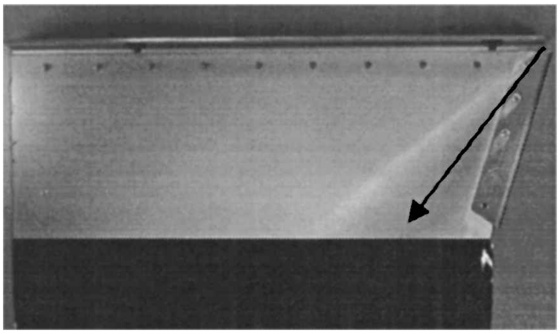

Fig. 5 C8 Earth end panel with bracket and rivets removed.

Solar absorptance and thermal emittance measurements were made on all five panels. The data were collected and plotted as shown in Fig. 6. The purpose of this plot was to evaluate the response space of the data and determine whether or not the data points were evenly distributed. There were two distinct groups of data. One set of data was associated with the 6061 CAA panels, and the other set of data was associated with the 6061 brackets that were not anodized.

Atomic Oxygen Fluence and Solar Exposures

Computer models were used to predict the atomic oxygen fluence and equivalent sun hours of solar exposure. These models included both direct flux and secondarily scattered flux to a given surface.[3] The atomic oxygen model included the thermal velocity spreading caused by the temperature of the upper atmosphere, shadowing of surfaces caused by the three-dimensional structure of the hardware, and the effect of the corotation of the atmosphere on the ram direction. The solar exposure model predicted the solar exposure defined as the effective number of hours of sunlight shining on a surface if the sunlight were striking normal to the plane of the surface. The solar model also included shadowing of surfaces caused by the three-dimensional structure of the hardware.

The solar exposure on the LDEF panels described in this report was caused by both direct radiation and secondary scattering. Vacuum UV wavelengths are less intense in scattered solar radiation than direct. Thus, the total solar exposure received on these panels was probably less damaging than if the exposure had been 100%

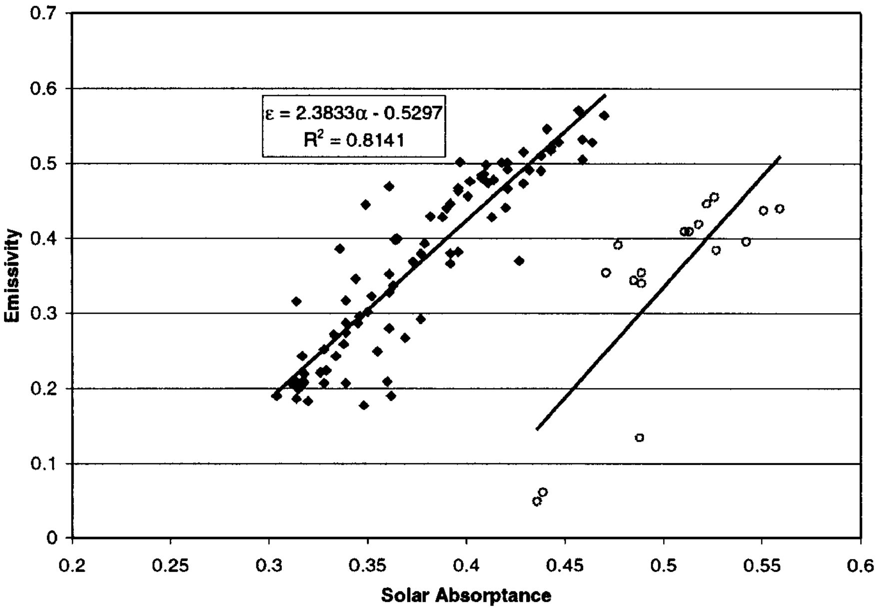

Fig. 6 Solar absorptance and thermal emittance data.

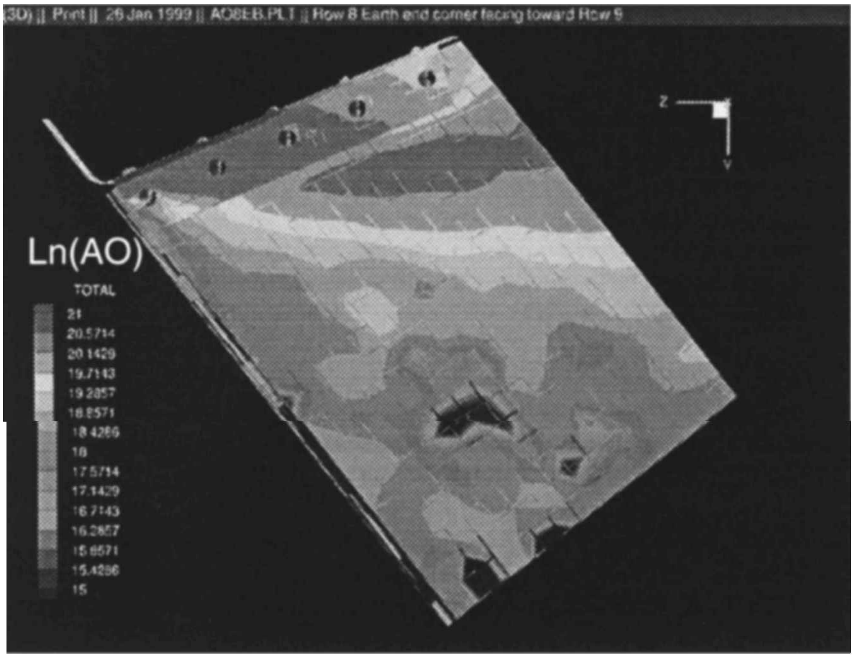

Fig. 7 AO fluence for C8 Earth end tray.

direct. Similarly, the atomic oxygen has a significant scattered component in the total fluence. Secondarily scattered atomic oxygen has given up some of its kinetic energy; however, atomic oxygen free radicals are still extremely reactive even with greatly reduced kinetic energy.

The LDEF tray overhangs shield much of the surfaces of interest from direct exposure. The geometry of LDEF is such that the outer surface of the tray walls are in close proximity to intercostals or longerons (within a few centimeters) that provide the surface to reflect the atomic oxygen and solar radiation. For the model calculations atomic oxygen or solar radiation was allowed to pass through a small (~2 × 2 cm) opening and either strike the LDEF tray surface or reflect from nearby structure. Actual opening sizes varied slightly from the model assumption. The atomic fluence to each surface was determined by integrating the flux determined at 6-min intervals over the entire mission (2106 days). The solar fluence calculation is a Monte Carlo calculation with results from all of the relative LDEF-sun positions possible during the mission summed to give the effective solar fluence.

Figure 7 is a surface plot of the logarithm of total atomic oxygen fluence received by the C8 Earth end panel over the entire mission. The areas of higher atomic oxygen fluence and thicker contaminant deposits appear to correspond with the darker areas of the contamination plume as shown in Figs. 8 and 9, respectively. For both figures the point of origin, and entry for atomic oxygen and solar UV, is in the upper-left-hand corner. Similar results with respect to atomic oxygen were observed for all five trays investigated in this work. Depth profile measurements were made on the C8 Earth end tray only.

Figure 10 is a similar surface plot of the total solar exposure across the C8 Earth end panel. On all of the trays analyzed, the brackets received considerably more solar exposure than the panels. On the panels the topography of the solar exposure is much flatter than that of the atomic oxygen fluence. Corresponding atomic oxygen

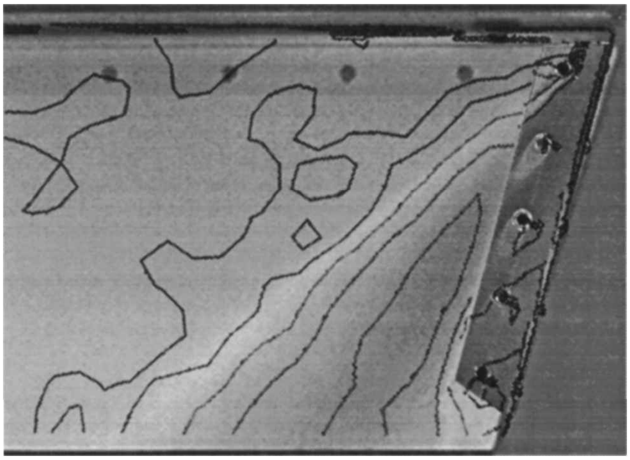

Fig. 8 Overlay of AO model onto photograph of C8 Earth end tray panel.

fluence and solar exposure values were determined for each optical property measurement location based on the model calculations.

Contamination Thickness Measurements

Detailed elemental depth profiles were produced for several points on the C8 Earth end using X-ray photoelectron spectroscopy measurements made in conjunction with controlled ion sputtering. Corresponding optical property measurements had previously been made at these same locations. The contaminant layer was assumed to extend from the surface down to the aluminum oxide. The aluminum oxide boundary point was defined for this work to be the point at which the aluminum and silicon concentrations intersected on the elemental depth profiles. Contaminant thickness determined in this manner ranged from 40 to 36,000 Å. Many of the depth profiles were characterized by a thin silicate crust with a layer of carbon-containing contaminant underneath. In areas where the contaminant was thin, only a silicate crust was present. In the past it has been presumed that silicone would be oxidized to silicate, leaving a clear, glassy crust. This evidence indicates that, while a

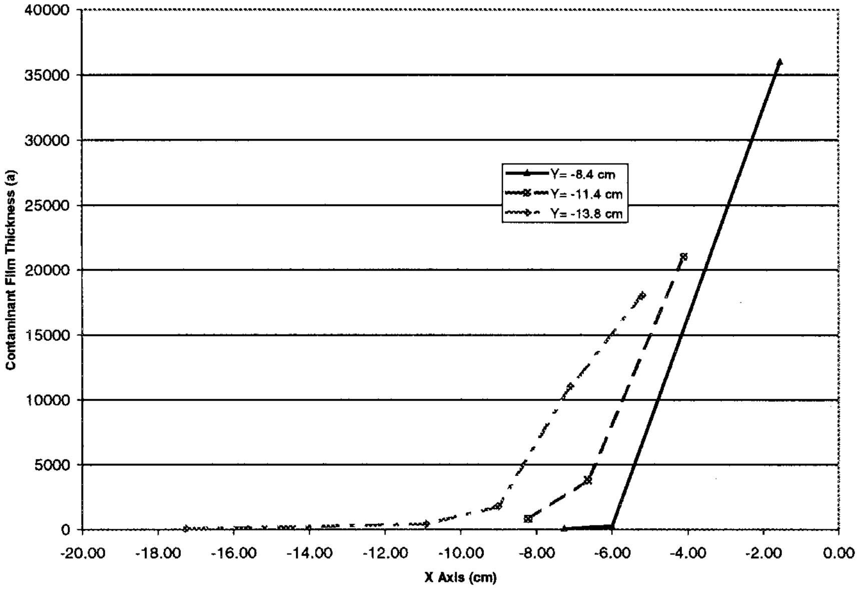

Fig. 9 Selected depth profile measurements as a function of position on C8 Earth end tray panel.

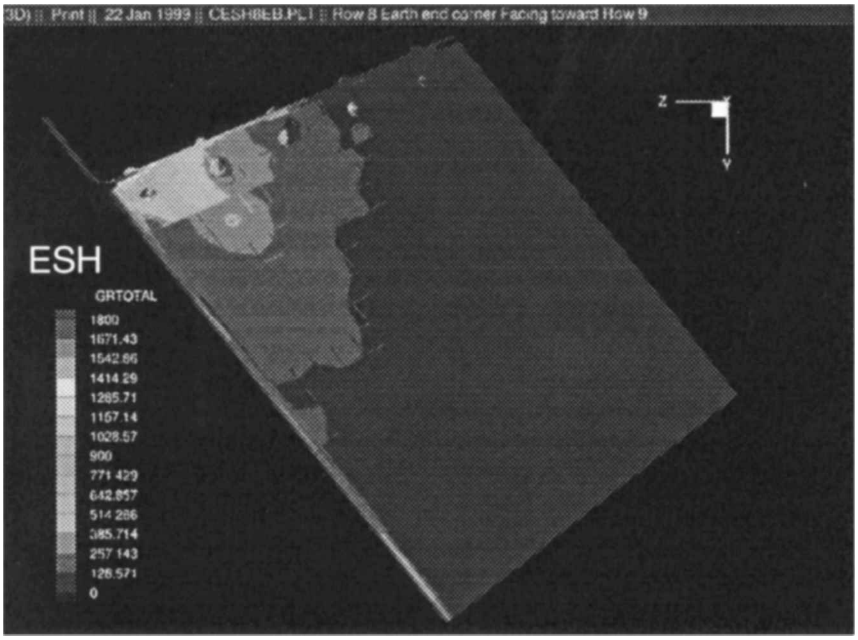

Fig. 10 Solar exposure for C8 Earth end tray.

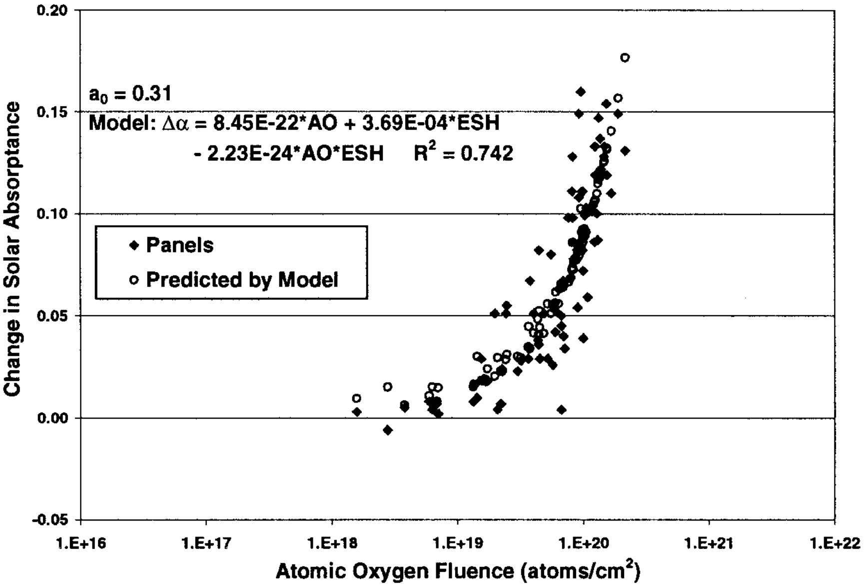

Fig. 11 Solar absorptance change vs atomic oxygen for panels.

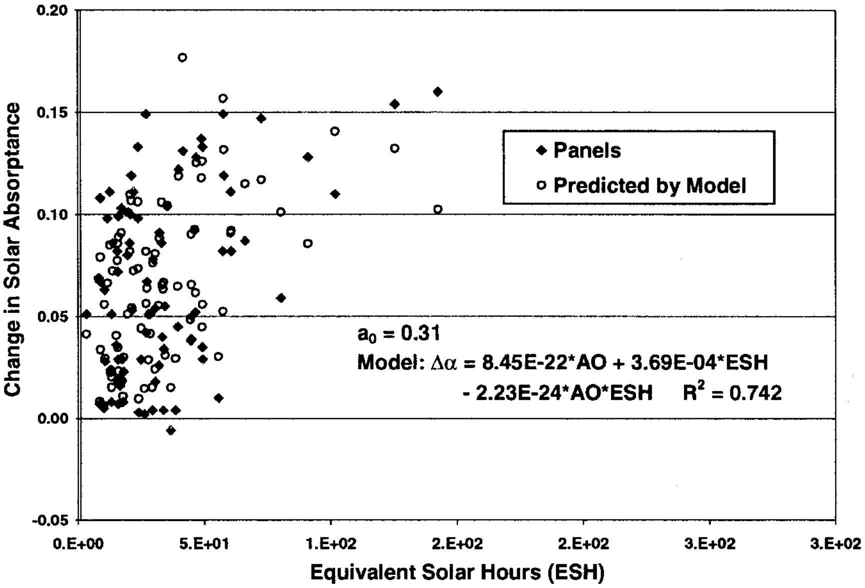

Fig. 12 Solar absorptance change vs solar exposure for panels.

silicate crust is formed, the formation of silicate can trap additional contaminant underneath, which can then darken under exposure to UV.

Regression Modeling

The optical property data, when plotted as shown in Fig. 7, clearly showed two separate populations of data. Based on this observation, the data sets from the panels and the brackets were modeled separately. Subsequent analysis showed that the 6061 panels were CAA, whereas the 6061 brackets were not.

The panel and bracket data from the five trays were modeled as functions of atomic oxygen fluence (AO, atoms O/cm^2) and solar exposure (equivalent solar hours). The data sets were linearized as necessary to explore various functional forms. Linear regression was then used to evaluate form suitability. It quickly became apparent that the changes in optical properties observed on these panels were a strong function of atomic oxygen and a weak function of solar exposure. The correlations improved when an interaction term was added. In fact, the interaction term is more significant than the solar exposure term by itself. Thus, the final functional form determined indicates that atomic oxygen is a major cause of optical property degradation and can act on its own. The solar exposure, on the other hand, is a weak factor that can cause more damage in the presence of atomic oxygen. The data and models for the panels are plotted in Figs. 11–13, and the models for the panels and the brackets are summarized in Table 2. In general, the least-squares correlation coefficient R^2 was observed to be higher for the solar absorptance models than for the thermal emissivity models. A good model fit is indicated by a correlation coefficient of 0.90 or greater. The coefficients for the optical property models that were based on environmental factors are between 0.68 and 0.82, implying that, while these models should not be used for accurate predictions, the models are following trends in the data.

Initial optical property data were not available. The values reported are the intercepts calculated from the regression modeling. The analysis shows that the optical properties are very material specific. For the same alloy surface treatment significantly affects solar absorptance and thermal emissivity. Surface treatment also affects the rate of optical property degradation. The atomic oxygen coefficients for panel models are twice those for the bracket models, indicating that the optical properties of the contaminated panels degraded twice as much as the contaminated brackets.

Table 2 Summary of regression model results

Surface	Initial optical property	Regression model	R^2
Panels	$\alpha_0 = 0.31$	$\Delta\alpha = 8.45 \times 10^{-22}$ AO $+ 3.69 \times 10^{-4}$ ESH[a] $- 2.23 \times 10^{-24}$ AO $\cdot$ ESH	0.74
(CAA 6061)	$\varepsilon_0 = 0.185$	$\Delta\varepsilon = 2.52 \times 10^{-21}$ AO $+ 1.26 \times 10^{-3}$ ESH $- 1.28 \times 10^{-23}$ AO $\cdot$ ESH	0.68
Brackets	$\alpha_0 = 0.41$	$\Delta\alpha = 4.42 \times 10^{-22}$ AO $+ 5.22 \times 10^{-4}$ ESH $- 3.20 \times 10^{-24}$ AO $\cdot$ ESH	0.82
(6061 only)	$\varepsilon_0 = 0.072$	$\Delta\varepsilon = 1.04 \times 10^{-21}$ AO $+ 2.28 \times 10^{-4}$ ESH $- 1.12 \times 10^{-24}$ AO $\cdot$ ESH	0.50
C8 panel	$\alpha_0 = 0.31$	$\Delta\alpha = 0.0277 \cdot \ln(\text{thickness}) - 0.143$	0.96
(CAA 6061)	$\varepsilon_0 = 0.185$	$\Delta\varepsilon = 0.0702 \cdot \ln(\text{thickness}) - 0.358$	0.99

[a] ESH = equivalent solar hours.

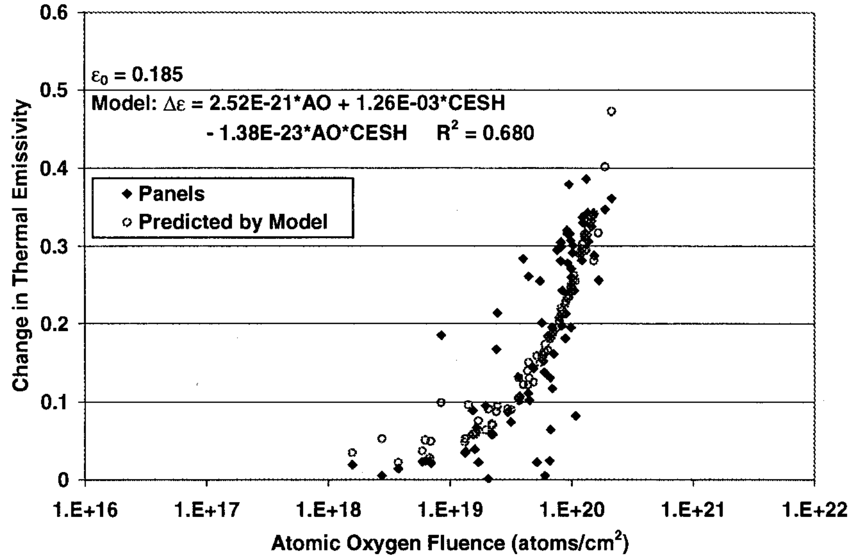

Fig. 13 Thermal emissivity change as a function of AO and ESH for panels.

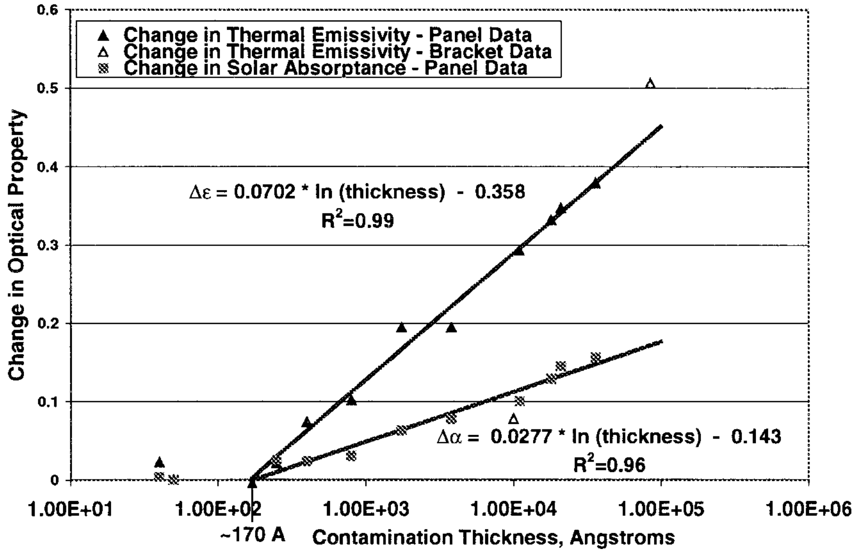

Fig. 14 Optical property changes as a function of contaminant thickness.

One criticism of this work might be that the models do not predict an asymptote for high levels of degradation. Current theory suggests that, once significant damage has occurred, the optical properties will stabilize. The nonlinear form of this work was chosen because the data fit well and because there was no evidence of an expected asymptote. Selection of one would have been highly speculative.

When the thickness data measured from panel C8 became available, attempts were made to incorporate the data into the existing atomic oxygen and solar exposure models. The correlations did not improve. Rather, it was discovered that models developed as a function of thickness alone (Fig. 14 and Table 2) produced excellent correlations (R^2 values greater than 0.95). It appears that the atomic oxygen and solar exposure and the intensity and view factor of the contamination sources interact to produce the thickness of the contaminant film. Atomic oxygen and solar exposure, in turn, interact with this film to produce darkening that determines the resulting optical properties. The analysis was confounded when all three variables were included.

The data and models in Fig. 14 suggest that a threshold thickness is required before significant changes in optical properties are observed. One explanation for this may be that the chromic-acid-anodized surface can absorb some contaminant into its pore structure before the contaminant will begin to build up on the surface and thus affect the optical properties.

Discussion

The discolored areas of contamination deposits on LDEF aluminum substrates were relatively thick. Discoloration occurred on both unanodized and the CAA 6061 aluminum surfaces LDEF. Areas of discoloration were contaminant mixtures that included both silicone-based and organic-based materials. The silicone contaminant was deposited preflight as a result of outgassing from the tray gasket material. The methyl silicone gasket was exposed to the tray exteriors for weeks to months, depending on the LDEF tray. The most likely organic sources are the Z306 black polyurethane binder paint that covered the lower half of the trays examined in this study, as well as Z306 covering longerons and intercostals in close proximity (within a few inches, direct line of sight) to the tray panels. Surfaces examined in this study had been sufficiently maintained after the flight such that potential artifacts were not a significant factor in the measurements.

In areas of the panel surface where the plume is visible, the composition of the contaminant layer is a coating of SiO_x several hundred angstroms in thickness covering a mixture of approximately 80% organic/20% silicone that ranged up to 36,000 Å thick. X-ray photoelectron sprectroscopy shows evidence of carbon-containing material present on contaminated surfaces extending far down into the anodized aluminum pore structure.

The substrate material was shown to have a significant effect on both the initial optical properties and the rate of optical property degradation. Models were constructed for 6061 and CAA 6061 aluminum to predict the optical property changes as a function of environmental exposure conditions. However, better predictions can be made using models that are based on contaminant thickness.

The change in solar absorptance with contamination thickness was approximately 0.06 per 1000 Å. A threshold contaminant thickness of approximately 170 Å was observed before any significant trend in solar absorptance change was evident. The 0.06 per 1000 Å change is less than the rate derived from earlier linear degradation models using temperature data telemetered from operational satellites, which have reported solar absorptance changes of 0.01 per 100 Å.

Emissivity changes for contaminated areas relative to values for uncontaminated substrate material were substantial. The change in thermal emissivity with contamination thickness was approximately 0.16 per 1000 Å. For the CAA surfaces the emissivity changed from 0.41 to as high as 0.56 for very thick deposits. On the corner brackets that were not anodized, the emissivity changed from 0.15 to around 0.50 for areas with extremely thick deposits (in excess of 15 μm). The initial values of emissivity for the panels and the corner brackets are caused by the different substrates. The reason for the difference in the postflight emissivity values or overall change in emissivity values is unknown. However, the atomic oxygen and solar exposures are known to have been more severe at the corner brackets, and the corner brackets most likely received more silicone preflight as the gaskets were located directly above.

There was a very high correlation between discoloration and atomic oxygen fluence. There was little correlation between solar exposure and discoloration. Only areas that received both atomic oxygen and solar UV were discolored. Previous work shows that, for the 6061 aluminum substrate, both anodized and bare, there was essentially no net buildup of contamination and no discoloration on surfaces exposed only to solar radiation (in some cases in excess of 11,000 equivalent sun hours).[2]

From the early shuttle flight experiments it was noted that atomic oxygen eroded organic paints and polymers such as Kapton®.[4–7] From those same experiments it was shown that atomic oxygen formed oxide layers on the surfaces of nickel, silver, and silicones. Little or no effect of atomic oxygen was seen on less reactive metals or oxidized material surfaces such as glass.

The contaminants on LDEF were a mixture of silicone and polyurethane-based materials. The silicone contaminant was deposited preflight as a result of outgassing from the tray gasket material. It is likely that the urethane from the Z306 outgassed both prior to flight and during the flight because the Z306 was painted on half of each tray panel and was present at all phases of the mission. It is quite possible that some or all of the urethane that was deposited during flight was then eroded away by the atomic oxygen, but all that is available to examine is the hardware at the end of the mission. Because the atomic oxygen flux level was very low during the early stages of the LDEF flight, it is also conceivable that there was some (or even considerable) diffusion of the urethane into the silicone prior to oxidation. Regardless of how the materials mixed together, the authors believe that the contaminant layer darkened as the layer continued to build up over time and as the trapped polyurethane molecules were exposed to, and broken down by, atomic oxygen and UV.

Although it is well documented that solar UV darkens contaminant films, the data refer to geosynchronous orbit environments where there is no atomic oxygen.[8–11] In LEO there is both atomic oxygen and solar UV. The LDEF data in this paper present strong evidence that atomic oxygen can have a greater impact on contaminant thickness and optical property degradation than solar UV does for this contaminant mix. A similar observation was made on LDEF by Rantanen et al. following the analysis of blanket vents.[12]

It is also well documented that atomic oxygen will erode UV-darkened organic films.[13,14] For example, this effect was demonstrated by taking specimens of A276 paint from LDEF trailing-edge locations where there was no atomic oxygen exposure and reflying these specimens in an atomic oxygen environment on the EOIM III space shuttle experiment. The darkened portion of the polyurethane binder from the UV exposure environment of the LDEF trailing-edge locations was virtually all removed by exposure to $\sim 2 \times 10^{20}$ atoms of oxygen/cm^2 on the space shuttle EOIM III experiment in 1992. If the contaminant film investigated in this paper had been polyurethane alone (i.e., no silicone), the film, if even formed, would have most likely eroded.

Conclusions

In LEO, it cannot be assumed that atomic oxygen will "clean away" contaminant films. This paper presents clear evidence that atomic oxygen can interact with "real life contaminants" to trap and build up contaminant films on surfaces rather than clean them. Also, solar UV is not the only, or even the most significant, darkening agent in LEO.

Acknowledgments

The authors would like to acknowledge the support of the Boeing ISS Program Contamination team and, specifically, Ron Mikatarian, Jim Visentine, and John Alred. We are grateful to NASA Langely Research Center for removing the LDEF panels from storage and for allowing us use of their laboratory during the initial stages. We would also like to thank AZ Technology for the use of their portable optical property instruments, the Laboratory Portable Spectro-Reflectometer (LPSR) 300 and the TEMP 2000 instrument, that were used to measure solar absorptance and thermal emittance, respectively.

References

[1] Levine, A. (ed.), "LDEF-69 Months in Space," *First Post-Retrieval Symposium*, Pt. 1, NASA CP 3134, June 1991, p. 3.

[2] Pippin, H. G., "Comparison of Spacecraft Contamination Models with a Well-Defined Flight Experiment," NASA CR-1998-208800, Final Rept., Sept. 1998.

[3] Levine, A. (ed.), "LDEF-69 Months in Space," *Second Post-Retrieval Symposium*, Pt. 1, NASA CP-3194, June 1992, p. 13.

[4] Leger, L., "Oxygen Atom Reaction with Shuttle Materials at Orbital Altitudes," NASA TM 58246, May 1982.

[5] Peters, P. N., Linton, R. C., and Miller, E. R., "Results of Apparent Atomic Oxygen Reactions on Ag, C, and Os Exposed During the STS-4 Orbits," *Geophysical Research Letters*, Vol. 10, No. 7, 1983, pp. 569–571.

[6] Kan, H. K. A., "Space Environment Effects on Spacecraft Materials," *Proceedings of Society of Photo-Optical Instrumentation Engineers: Radiation Effects in Optical Materials*, edited by P. W. Levy, Vol. 541, SPIE—The International Society for Optical Engineers, Bellingham, WA, 1985, pp. 164–180.

[7] Visentine, J. (ed.), "Atomic Oxygen Effects Measurements for Shuttle Missions STS-8 and 41-G," NASA TM 100459, Vol. 1–3, Sept. 1989.

[8] Hyman, N. L., "Solar Absorptance Degradation of an Uncleaned Radiator," *Comsat Technical Review*, Vol. 11, No. 2, 1981, p. 433.

[9] Anderson, C. C., and Hajjar, M. M., "Calorimetric Measurements of Thermal Control Surfaces at Geosynchronous Orbit," AIAA Paper 87-1571, June 1987.

[10] Stewart, T. B., Arnold, G. S., Hall, D. A., Marvin, D. C., Hwang, W. C., Owl, R. C. Y., and Marten, H. D., "Photochemical Spacecraft Self-Contamination Laboratory Results and System Impacts," *Journal of Spacecraft and Rockets*, Vol. 26, No. 5, 1989, p. 358.

[11] Arnold, G. S., and Luey, K., "Photochemically Deposited Contaminant Film Effects," *Proceedings of the Society of Photo-Optical Instrumentation Engineers: Optical System Contamination V and Stray Light and System Optimization*, edited by A. P. M. Glassford, R. P. Breault, and S. M. Pompea, Vol. 2864, SPIE—The International Society of Optical Engineers, Bellingham, WA, 1996, pp. 269–285.

[12] Rantanen, R. T. G., Finckenor, M., and Pippin, H. G., "Comparison of Contamination Model Predictions to LDEF Surface Measurements," *Proceedings of the Society of Photo-Optical Instrumentation Engineers Conference on Optical System Contamination: Effects, Measurements and Control VI*, Vol. 3427, SPIE—The International Society of Optical Engineers, Bellingham, WA, 1998, p. 260.

[13] Jaggers, C. H., and Meshishnek, M. J., "Exposure of LDEF Materials to Atomic Oxygen: Results of EOIM III," LDEF-69 Months in Space, *Third Post-Retrieval Symposium*, Pt. 3, NASA CP 3275, Nov. 1993, p. 931.

[14] Golden, J. L., Bourassa, R. J., Dursch, H. W., and Pippin, H. G., "Analysis of Selected Specimens from the STS-46 Energetic Oxygen Interaction with Materials-III Experiment," LDEF-69 Months in Space, *Third Post-Retrieval Symposium*, Pt. 3, NASA CP 3275, Nov. 1993, p. 1067.

A. C. Tribble
Associate Editor